Responses of *Ceriodaphnia dubia* to TiO$_2$ and Al$_2$O$_3$ nanoparticles: A dynamic nano-toxicity assessment of energy budget distribution

Minghua Li[a], Kirk J. Czymmek[b], C.P. Huang[a],*

[a] *Department of Civil and Environmental Engineering, University of Delaware, Newark, DE 19716, USA*
[b] *Department of Biological Sciences, Delaware Biotechnology Institute, Delaware Technology Park, Newark, DE 19711, USA*

ARTICLE INFO

ABSTRACT

The in vivo responses of *C. dubia* to nanoparticles exemplified by a photoactive titanium oxide (TiO$_2$) and a non-photocatalytic aluminum oxide (Al$_2$O$_3$) were studied. Both nanomaterials inhibited the growth of *C. dubia* at concentrations ca. >100 mg/L. The EC50 value was 42 and 45 mg/L in the presence of TiO$_2$ and Al$_2$O$_3$, respectively, based on 3-brood reproduction assay. Results implied that reactive oxygen species (ROS) may not be totally responsible for the adverse effects exerted on the invertebrate. Aggregation and interaction among nanoparticles, *C. dubia*, and algal cells, major food source of *Daphnia*, played a significant role on the responses of *C. dubia* to nanoparticles. Dynamic energy budget (DEB) analysis was used to assess the impact of nanoparticles on the energy allocation of *C. dubia*. Results indicated that nanoparticles could disrupt the assimilation and consumption of energy in *C. dubia* dramatically. The assimilation energy was negatively correlated to the concentration of nanomaterials, a reduction from 11 to near 0 µg-C/animal/day in the presence of TiO$_2$ or Al$_2$O$_3$ nanoparticles at a nanoparticle concentration of 200 mg/L. The energy consumed for life-maintenance increased also with increase in the concentration of nanomaterials. Results clearly demonstrated the importance of energy disruption in determining the toxicity of nanoparticles toward *C. dubia*.

1. Introduction

Increasingly, nanomaterials have received much attention in many fields, e.g., catalysis, sensors, and electronics. Given the increasing production of nanomaterials worldwide, the potential for their release into the environment thus posing subsequent impacts on ecological health have become a great public concern. With uniquely small size, nanomaterials can be highly reactive, ideal for many beneficial industrial uses and potentially high risk to the environment. There are increasing research activities focusing on the adverse effects of various engineered nanomaterials on human and environmental health [1,2]. While the major toxicity mechanism of most nanomaterials has not yet been elucidated completely, possible causes such as membrane disruption, oxidation of proteins, genotoxicity, interruption of energy transport, formation of reactive oxygen species (ROS) and the release of toxic constituents (i.e., secondary toxicity) have been suggested [1,2].

Many research groups have reported that exposure to nanoparticles could cause oxidative stress in cells at the cellular and subcellular levels [1,2]. The ROS generated by nanomaterials can damage the cell membrane indirectly by oxidizing the double bonds of the fatty acid tails in membrane, i.e., lipid peroxidation, as well as cause lesions in proteins and DNA and disulfide formation [2,3].

In as much as the commonly speculated mechanisms of inflicting adverse effects on target organisms by ROS, most toxicity studies have been carried out in vitro at the cellular level [2]. Current literature is still debating on the link between nanoparticles, oxidative stress and toxicity using in vivo invertebrates and vertebrates toxic assays. Results of one early study by Oberdorster showed that fullerene (C60) could generate ROS which subsequently damaged the brain of largemouth bass; however, only one of nine tests showed positive response to ROS oxidation [4]. It was also reported that the presence of nanoparticles, including Ag, Au and C60, caused oxidative stress to various aquatic animals [5–8]. However, conflicting results were also reported in literature. Later in vivo toxicity study of C60 using fathead fish and medaka by Oberdorster et al. [9] failed to prove protein or DNA damage or cellular oxidation responses. Shinohara et al. [10] reported that C60 exposure did not induce any lipid peroxidation of the brain tissue of *C. carpio* in vivo. Henry et al. [11] concluded that trace solvent residues such as tetrahydrofuran, used in the preparation of C60 fine suspensions, and its degradation products were neuro-toxicants that could be responsible for damaging the brain of largemouth bass. In summary, the exposure pathways of most nanomaterials and toxi-

* Corresponding author. Tel.: +1 302 831 8428; fax: +1 302 831 3640.
E-mail address: huang@ce.udel.edu (C.P. Huang).

city mechanisms remained largely speculative. Furthermore, most current nanotoxicity studies that followed the conventional protocols specifically designed for dissolved chemical species may not be totally applicable to solid nanomaterials.

In addition to the direct chemical stresses, other factors such as food availability, energy assimilation and allocation may also impact the target organisms in the presence of nanomaterials. Energy is essential for all living systems and its allocation is a dynamic process that may vary with ecological fluctuations, such as food availability, temperature, pollutants, and the population per se. The presence of nanomaterials can change the environmental settings, which can affect the physiological and physical fitness of testing organisms. Hence, the adverse effects observed in vivo might be partially attributed to the disruption of energy budget. The energy budget model that correlates the energy essential for life cycle activities such as growth, development, and reproduction with environmental variables can be a useful tool to quantify the energy uptake and allocation in biological systems in the presence of nanomaterials.

The objectives of the present research were: (a) to assess the role of photocatalysis on the responses of C. dubia to nanoparticles exemplified by photoactive TiO_2 P25 and non-photocatalytic γ-Al_2O_3, (b) to investigate the effects of nanoparticles on factors such as food availability and body burden that may affect energy balance of C. dubia, and (c) to analyze the energy budget of C. dubia exposed to selected nanomaterials and its relationship to observed toxic responses.

2. Experimental

2.1. Nanoparticles

Degussa TiO_2 P25, purchased from Degussa Co., (Parsippany, NJ, USA), contains approximately 70% anatase and 30% rutile. The TiO_2 P25 is known to have high photoactivity and generate ROS when exposed to light. Commercial γ-Al_2O_3, supplied by Degussa Co., was selected as typical non-photocatalytic nanomaterials. The properties of nanoparticles were characterized for primary particle size, aggregate (or secondary particle) size, specific surface area and surface charge, i.e., pH_{zpc}. The primary particle size was determined with transmission electron microscopy (TEM) (JEOL JEM-2000FX) and a value of 34 and 17 nm for TiO_2 P25 and γ-Al_2O_3, respectively, was obtained. The particle suspensions were dispersed with ultrasound for 30 min in deionized water (DW) or in moderately hard water (MHW) at pH 7, respectively, then the aggregate size of nanoparticles, (or the secondary particle size) was determined with dynamic light scattering (DLS) using Zeta-Sizer 3000HSa (Marvin Instrument). The aggregate size was ~200 and ~100 nm in DW and ~2000 and ~200 nm in MHW at pH 7, for TiO_2 P25 and γ-Al_2O_3, respectively. Results of the aggregation kinetics of various TiO_2 nanoparticles in MHW will appear elsewhere later [12]. It was also worthy to point out that the interaction between nanoparticles and surrounding media, including algal cells, played an important role on the concentration of nanoparticles [13,14]. Thus, the actual exposure concentrations were not a constant in most in vivo nanotoxic assays [14]. Direct comparison of the assay outcome might not be straight forward, as the actual exposure concentrations varied as a function of nanoparticle properties, surface functionality, time, solution ionic strength, pH and ionic composition [14–18]. The dynamic aspect of actual nanoparticle concentration in various assay media should be studied in a systematic manner.

The surface charge was characterized in terms of pH_{zpc} and zeta potential measurements in MHW using ZetaSizer 3000HSa (Marvin Instrument). At pH 7 in MHW, the zeta potential was −10 and 15 mV for TiO_2 P25 and γ-Al_2O_3, respectively. The pH_{pzc} (point of zero charge) was 5.5 and 8.9 for TiO_2 P25 and γ-Al_2O_3, respectively. The zeta potential for TiO_2 and Al_2O_3 were comparable to literature data with slight deviation for Al_2O_3 [14], which was likely due to the difference in the crystal structure of the nanoparticle, solution chemistry, specifically ionic strength and pH, in addition to possible experimental errors [15]. The specific surface area was determined based on the Brunauer–Emmett–Teller multilayer nitrogen gas adsorption (BET) theory (NOVA2000, Quantachrome Corp) and a value of 47.7 and 89.8 $m^2\,g^{-1}$ for TiO_2 P25 and γ-Al_2O_3 respectively was obtained. The surface properties and aggregate size of the nanoparticles were summarized in supplemental material (Table S1).

2.2. Cultivation of organisms

Unicellular green algae, Selenastrum capricornutum (renamed as Pseduokirchneriella subcapatitata), and the cladocerans, C. dubia, cultures were purchased from Aquatic Biosystems Inc. (Fort Collins, CO, USA). C. dubia were cultured according to U.S. EPA guidelines in synthetic MHW [19]. In brief, all C. dubia were incubated in the growth chamber inside of a climate control room with 16-h light/8-h dark photoperiod at room temperature of $26 \pm 0.3\,°C$.

"All the experiments were carried out at light intensity of 1200 lx using GE plant aquarium wide spectrum light bulbs to simulate the solar light source (Fig. S3). These light fixtures provided output in the UV region i.e., (below 400 nm). Thus, the light source ensured the photoactivities of TiO_2 P25 nanoparticles which band gap is 3.0–3.2 eV (or corresponding to wavelength of 380–400 nm). Consequently, the generation of ROS was expected."

2.3. Growth assay

A dose–response growth assay was conducted on C. dubia in order to evaluate the sub-lethal effects of nanomaterials. C. dubia neonates (age difference <4 h) from the same brood board were randomly distributed into a series of culture beakers containing 200 mL of growth medium with nanoparticles in the concentration range of 10–200 mg/L (ppm) for both nanomaterials. Every 24 h, C. dubia neonates were transferred to new growth chambers containing freshly prepared nanoparticle suspensions at the same initial concentrations. Food was added to the fresh medium immediately after the adults were transferred to new growth chambers. Each feeding consisted of 0.1 mL of YCT and 0.1 mL of Selenastrum capricornutum concentrate per 15 mL of test solution (note: 0.1 mL of algal concentrate containing 3.0–3.5×10^7 cells/mL yielded 2–2.3×10^5 cells/mL in the test chamber upon dilution). After 48 h, all living neonates were recovered and the body length of individual C. dubia were recorded under Olympus AX70 microscope ($100\times$) (Olympus America Inc.). The individual C. dubia was documented photographically and images were processed using the software, Image-Pro plus (Media Cybernetics, Inc.).

2.4. Reproduction assay

The 3-brood reproduction test was performed according to EPA Method 1002 with slight revision [19]. Neonates less than 24 ± 4 h of age were used. The exposure concentrations were in the range from 5 to 100 mg/L for both nanoparticles. Freshly prepared solutions were used to renew the assay daily. The C. dubia was fed daily immediately after transfer to new suspension with the same food concentration as indicated above. The total number of young C. dubia produced in the first 3-broods was summed. Reproduction data obtained from the chronic tests were used to calculate the EC50 values by point estimation technique. Toxicity Relationship Analysis Program version 1.00 (TRAP) from the national health
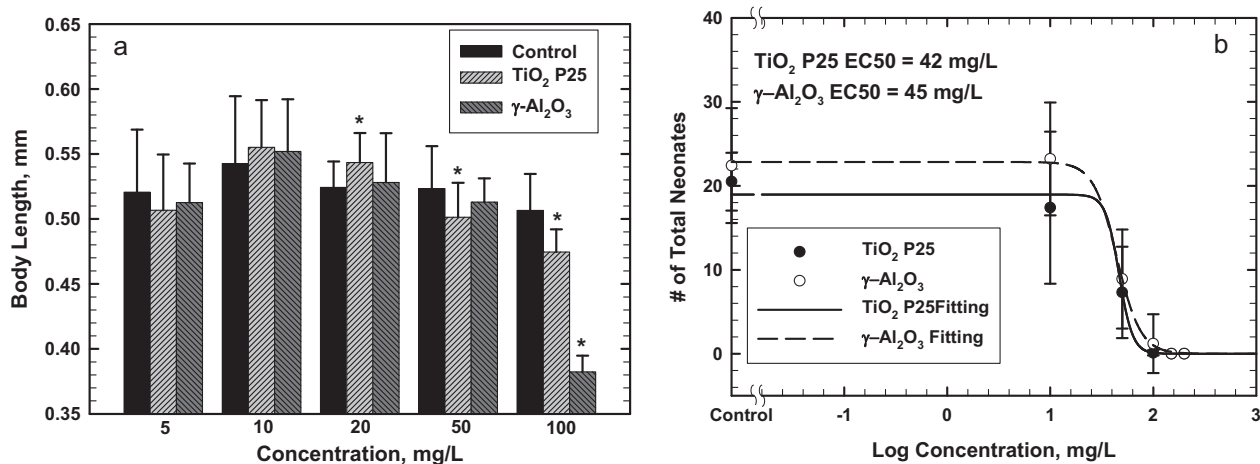
Fig. 1. (a) The body length of *C. dubia* after 48 h of exposure to TiO$_2$ P25 and γ-Al$_2$O$_3$ of various concentrations (*significantly different from the control, ANOVA, $p < 0.05$), and (b) dose–response curves of *C. dubia* of three-brood reproduction tests in the presence of TiO$_2$ and γ-Al$_2$O$_3$ nanoparticles.

and environmental effects research laboratory (NHEERL) of U.S. EPA was used to analyze the data.

2.5. Distribution of nanomaterials

The distribution of nanoparticles inside the animal body after exposure was investigated by a whole mount confocal microscopy and a resin filtration and embedment method. For live *C. dubia* imaging, samples were placed in a single-well (no 1.5 Nalge Nunc chamber-cover glass system) and observed under either a Zeiss LSM 5 DUO or LSM 510 NLO confocal microscope. The 488-nm laser line of an Argon ion laser (25 mW) was used for excitation of autofluorescence and reflected light simultaneously with a 505-nm long pass emission filter and 475-nm long pass emission filter, respectively. Due to the optical opacity of dense aggregates of nanomaterials, in order to visualize more clearly internal structures, resin embedding and sectioning were used to produce *C. dubia* slides for examination.

2.6. Algal cells concentration

An assay was conducted to quantify the algal concentrations available to *C. dubia* after exposure to nanoparticles. Culture cups (30 mL in volume) filled with 15 mL of MHW used to conduct the 3-brood reproduction and the 24-h acute assay were employed here to reproduce the true algal cell concentrations in those assays. Pre-determined *Selenastrum capricornutum* stock solution was added to the cup yielding a 2×10^5 cell/mL of initial concentration. A pre-determined amount of TiO$_2$ and Al$_2$O$_3$ stock solution was added to the culture cup followed by proper dilution with MHW to produce a series of exposure concentrations. The suspension was left stand still as in the 3-brood reproduction assay in the constant temperature room. After a 24 h of exposure, 1 mL of the suspension was taken from the upper portion of each culture cup and transferred into 15-mL centrifuge tube. The centrifuge tubes were refrigerated at 4 °C until further analyses for the algae density using an Olympus microscope AX70 and hemocytometer. Each sample was counted at least four times. At least five replicates were tested for each concentration or nanoparticles.

3. Results and discussion

3.1. Growth and reproductive responses

Fig. 1a shows the body length of *C. dubia* after 48 h of exposure to the selected nanoparticles at various concentrations. In each test

concentration, about 15 *C. dubia* neonates were cultured in the test suspension at the onset of each experiment. All survived and intact *C. dubia* were used to calculate the average body length. ANOVA single factor analysis was performed to determine if the treated group was significantly different from that of the control group using a p value of 0.05. The average body length of *C. dubia* in 5 control groups (total of 85 individuals) was 0.52 ± 0.04 mm after 48 h of exposure. Results indicated that both nanomaterials delayed the development or growth of *C. dubia* at concentration of 100 mg/L. It is interesting to note that although TiO$_2$ P25 is known to have high photo-catalytic capability, its inhibitory effect is similar to that of Al$_2$O$_3$, which is not photosensitive. Over the concentration range studied, both TiO$_2$ and Al$_2$O$_3$ had similar impact on the growth of *C. dubia*. Surprisingly, at the concentration of 100 mg/L, Al$_2$O$_3$ reduced the body length of *C. dubia* significantly than TiO$_2$ P25. The average body length was 0.38 mm in the presence of Al$_2$O$_3$ versus 0.47 mm when TiO$_2$ nanoparticles were present.

Fig. 1b shows the dose–response curve assessing the long-term effect of nanoparticles on neonates in 3-brood reproduction assay. Consistent with the above growth tests, TiO$_2$ P25 and Al$_2$O$_3$ yielded no significant difference in reproductive capability at the 95% level by ANOVA analysis with an EC50 value of 42 and 45 mg/L, respectively, although TiO$_2$ is highly photo-active and Al$_2$O$_3$ is not.

The growth of *C. dubia* was delayed significantly at concentration of 100 mg/L for both nanoparticles. At concentrations of 50 mg/L, TiO$_2$ nanoparticles delayed the growth of *C. dubia* by 4.2% and Al$_2$O$_3$ nanoparticles showed no effects compared to control group. In contrast, *C. dubia* suppressed reproduction by approximately 50% at concentration of 50 mg/L, suggesting *C. dubia* allocated limited energy source for growth rather than reproduction, a survival strategy under adverse conditions prioritizing its energy allocation in response to environmental stress. Both results of reproduction and growth assays indicated that there was no difference in toxic responses between photoactive TiO$_2$ and non-photoreactive Al$_2$O$_3$. This suggested that the generation of ROS was not the major stress for *C. dubia*. Rather other factors such as interactions among nanoparticles, algal cells and *C. dubia* and associated impacts on the animals should be considered.

3.2. Distribution of nanoparticles

The distribution of nanoparticles in adsorbed, trapped, or ingested state on *Daphnia* was visualized first using confocal microscope. The technique allows direct observation of the responses of *C. dubia* to nanoparticles in situ. These real-time images represent
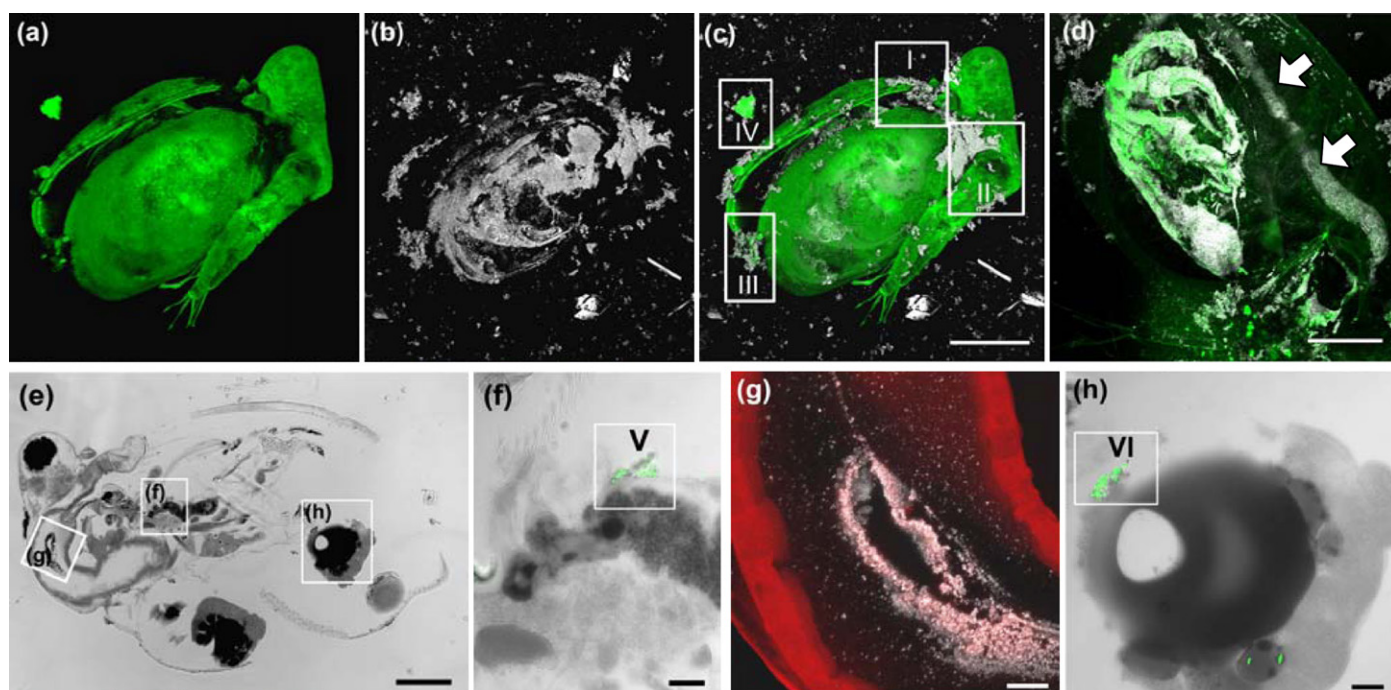
Fig. 2. (a)–(d) The 3D confocal images of representative *C. dubia* exposed to 50 mg/L of TiO$_2$ with 2-h exposure time. (a) The fluorescent (green) image of *C. dubia*, (b) the reflection (white) image of TiO$_2$, (c) combination of the reflection (white) and fluorescent (green) channels: I, TiO$_2$ attached on and under the carapaces; II, TiO$_2$ clusters accumulated on the joints; III, TiO$_2$ particles attached to the abdominal appendages; IV, TiO$_2$ and algal cells clusters in the suspension, and (d) another *C. dubia* with digestive tract full of TiO$_2$ particles. (e) and (f) Confocal images of *C. dubia* exposed to TiO$_2$ fixed in resin and sliced in sections. (e) Transmitted light image of the *C. dubia* section showing the oblique section of the digestive tract. See the enlarged frames of (f)–(h) in their corresponding panels below. (f) Mix of the transmitted light, resin and TiO$_2$ reflection signal (green). TiO$_2$ particles attached to the tissue of *C. dubia* (V). (g) 3D confocal images of reflective TiO$_2$ particles (white) in the digestive tract tissues (red) and (h) egg in the brood chamber with attached TiO$_2$ particles (VI). (c)–(e) scale bar = 100 μm, (f)–(h) scale bar = 10 μm. (For interpretation of the references to color in the text, the reader is referred to the web version of the article.)

the most direct visualization of how nanomaterials interact with the living *C. dubia* and vice versa.

Fig. 2 shows the typical 3D confocal images of *C. dubia* exposed to TiO$_2$ nanoparticles. The nanoparticles were found trapped inside and/or on the carapaces of *C. dubia* (Fig. 2c, I), accumulated between the joints (Fig. 2c, II), and/or attached to the area of abdominal appendages. It was also noted that the nanoparticles were able to attach to algal cells and formed large aggregates as shown in Fig. 2c, IV. The physical interaction between nanoparticles and algal cells was crucial to the colloidal stability of the nanoparticles and the concentration of free algal cells in the growth media. Results showed that a thick layer of TiO$_2$ nanoparticles were adsorbed on the algae cell surface in the presence of TiO$_2$ nanoparticles at concentration in the range of 10–100 mg/L (Fig. S3). Large TiO$_2$–algae agglomerates in the range of 6–45 μm were formed and settled readily [18]. Thus, it must be noted that the concentrations of both nanoparticles and algal cells could be affected. TiO$_2$ nanoparticles were also found in the digestive tract of *C. dubia* as seen in Fig. 2d (white tract as indicated by the arrows).

Resin embedding and sectioning technique, which chemically fixates and transfers biological materials into a cross-linked matrix and preserves the physical integrity of cellular components, was chosen to reveal the interaction between the internal organs and the nanoparticles. Fig. 2e–g presents typical confocal images of resin embedded and semi-thick sectioned (~10 μm thick) *C. dubia* exposed to nano TiO$_2$ particles. The TiO$_2$ nanoparticles were found in the digestive tract (Fig. 2g), tissues (Fig. 2f), brood chambers (Fig. 2h), and appendages. It is also noted that, though a large quantity of TiO$_2$ nanoparticles were present in the gut, the good shield of the gut wall retained them securely without particle leakage as no TiO$_2$ signal (white) appeared outside the gut wall (Fig. 2g). This suggested that the nanoparticles were not able to penetrate the gut wall after they were ingested. With the assistance of imaging tools, it is possible to propose preliminary exposure pathways of nanoparticles to filter-feeding organisms such as *C. dubia*: direct contact, ingestion, and internal tissue/embryo contacts.

3.3. Dynamic energy budget (DEB) model

To quantify the overall energy budget of *C. dubia* in the presence of two nanoparticles, the DEB model was applied, which successfully predicted the life history of an animal under various environmental conditions, such as food availability, temperature, and population density [20–23]. According to the DEB model, the food ingested (*I*) and assimilated (*A*) by an animal is used for life-support functions, i.e. maintenance (*M*), storage/growth (*S*), and reproduction (*R*) [22,24,25]. For a closed biological system, the overall energy balance can be summarized as Eq. (1) [22,24,25]:

$$A = M + S + R \tag{1}$$

Detailed DEB methodology, model equations and parameters are summarized in Tables S2 and S3 respectively in supplemental material.

Algal cells, as the only food source, are crucial to *C. dubia* energy assimilation. The quality and density of algal cells are known to influence the energy assimilation rate, subsequently affecting the development, fitness and reproduction of *C. dubia* [22,24,25]. The culture medium, consisting of various monovalent and divalent ions, can lead to the aggregation of nanoparticles followed by particle destabilization. In the meantime, the nanoparticle aggregates interact with the algal cells, forming clusters as shown in Fig. 2. Thus, the quality and the quantity of the algal cells were subsequently impaired.
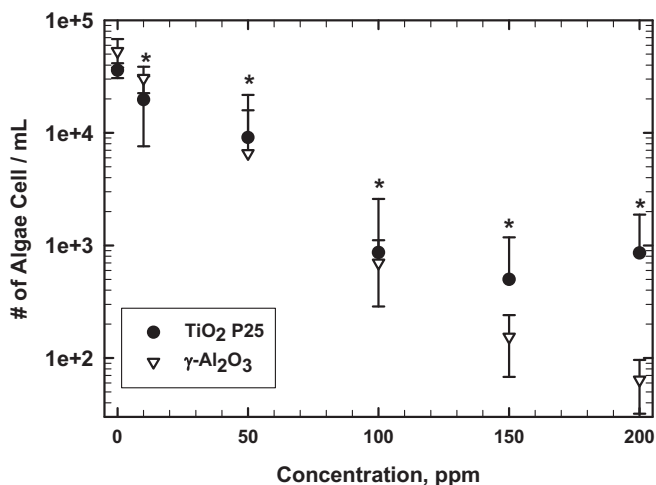
Fig. 3. Algal cell concentrations after 24 h exposure to various concentration of TiO₂ P25 and γ-Al₂O₃ (*significantly different than control, ANOVA, $p < 0.05$).

Results indicated that the algal cell concentration was reduced by about 1000 times in the presence of 200 mg L⁻¹ of γ-Al₂O₃ (Fig. 3), which reduced assimilation energy consequently. The algal cell concentration was reduced from 5×10^4 to 64 cell/mL and from 5×10^4 to 860 cell/mL in the presence of 200 mg/L of γ-Al₂O₃ and TiO₂ P25, respectively. This suggested that the food source available to *C. dubia* was influenced significantly by the presence of both nanoparticles, which subsequently influence the energy uptake of the *C. dubia*.

The ingestion rate and assimilation rate of 7-day *C. dubia* exposed to nanomaterials at various concentrations were first modeled based on the measured algal density (Fig. 3). The body weight used in the model was measured as described in Table S4 (supplemental material) and a scaling factor of 0.42 was used to convert the body weight to body carbon content [23,26]. Fig. 4 shows the predicted ingestion rate (I), energy assimilation rate (A), and assimilation efficiency (E_A) as a function of nanoparticle concentration.

Both nanoparticles exhibited quite similar trends in the energy assimilation rate of *C. dubia*. The predicted ingestion rate decreased from 20.1 to 3.4 μg-C/animal/day as the concentration of TiO₂ nanoparticles increased from 0 (i.e., control) to 200 mg/L. For γ-Al₂O₃ nanoparticles; the ingestion rate was reduced from 20.1 to 0.3 μg-C/animal/day when the particle concentration was

increased from 0 (of control) to 100 mg/L. Also, there was marked reduction in the assimilation energy rate in the presence of nanoparticles, a decrease from 11.0 to 2.9 and from 11.0 to 0.3 μg-C/animal/day in the presence of 200 mg/L of TiO₂ and Al₂O₃, respectively.

It was noted that there was a large difference between the rate of ingestion energy and assimilation energy at low particle concentration (or high food concentration). Apparently the organism can adjust its assimilation efficiency (E_A) automatically [27,28]. A negative correlation between energy assimilation efficiency and food availability was the common strategy to maximize energy capture [27,28]. Therefore, at high nanoparticle concentrations (or food scarcity), the animals tend to increase their assimilation efficiency.

Another factor, critical to the fitness of organisms is body weight. Adsorption of nanoparticles physically increased the body burden of *C. dubia*. Hence, the corresponding maintenance expenditure increased accordingly. Fig. 4 also shows the predicted maintenance energy in the presence of nanomaterials at various concentrations. The energy allocated to maintenance increased slightly with increase in the concentration of nanomaterials. The maintenance expenditure was ca. 3.4 μg-C/animal/day without nanoparticles and increased to 5.0 and 4.2 μg-C/animal/day in the presence of 200 mg/L of TiO₂ P25 and γ-Al₂O₃, respectively.

Food availability has not been explored in most current nanotoxicity studies. The total energy captured by an organism is essential to life support and is dependent on the availability of foods. The presence of nanomaterials can deplete food supplies due to interactions between nanoparticles and foodstuffs, such as by adsorption, and aggregation and destabilization of particles. Even the presence of small amounts of electrolytes in the growth media, such as the MHW commonly used in the EPA toxicity testing protocols, can induce aggregation and sedimentation of nanoparticles, as well as the depletion of biologically accessible food sources or nutrients. Reduction of food supply is known to delay the development and growth of animals and inhibit their reproduction ultimately. Many researchers have reported a positive relationship between the food availability and body length and weight [28,29]. For example, at a food concentration of 1.0 mg-C/L, the average body length of 10-day old *D. galeata* was 2.1 mm, which was reduced to 1.6 mm when the food concentration was diluted by 10 times to 0.1 mg-C/L [28]. The measured algal cells concentration and simulation results indicated that the energy uptake of *C. dubia* was disrupted due to the presence of nanoparticles, which contributed to the growth delay observed.
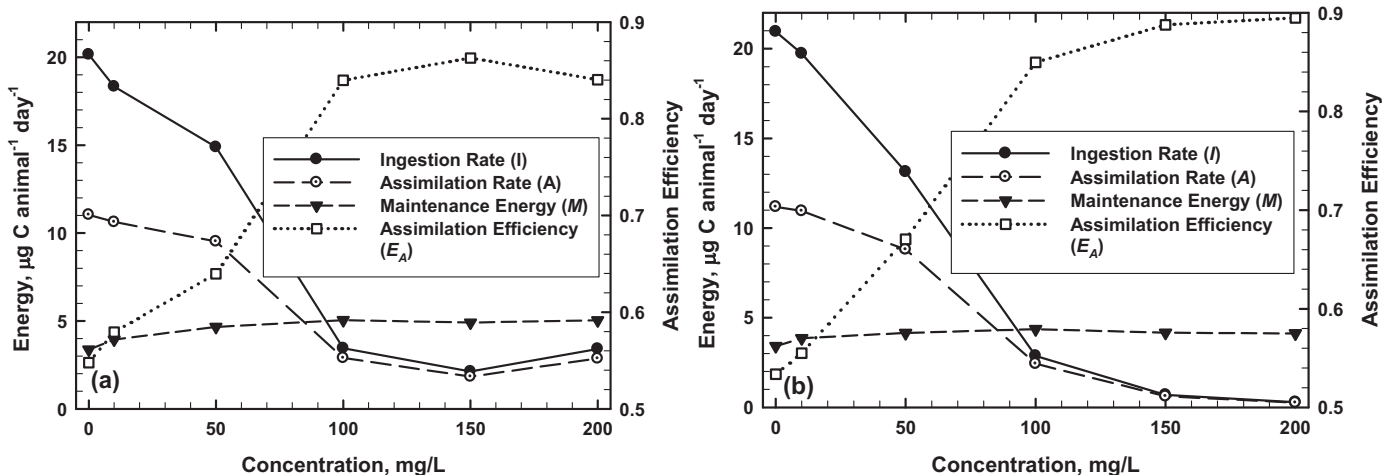

Fig. 4. The energy capturing [ingestion rate (I) and assimilation rate (A)] and expenditure rate [maintenance energy rate (M)] of *C. dubia* as a function of nanoparticle concentration in the presence of (a) TiO₂ P25 and (b) γ-Al₂O₃.
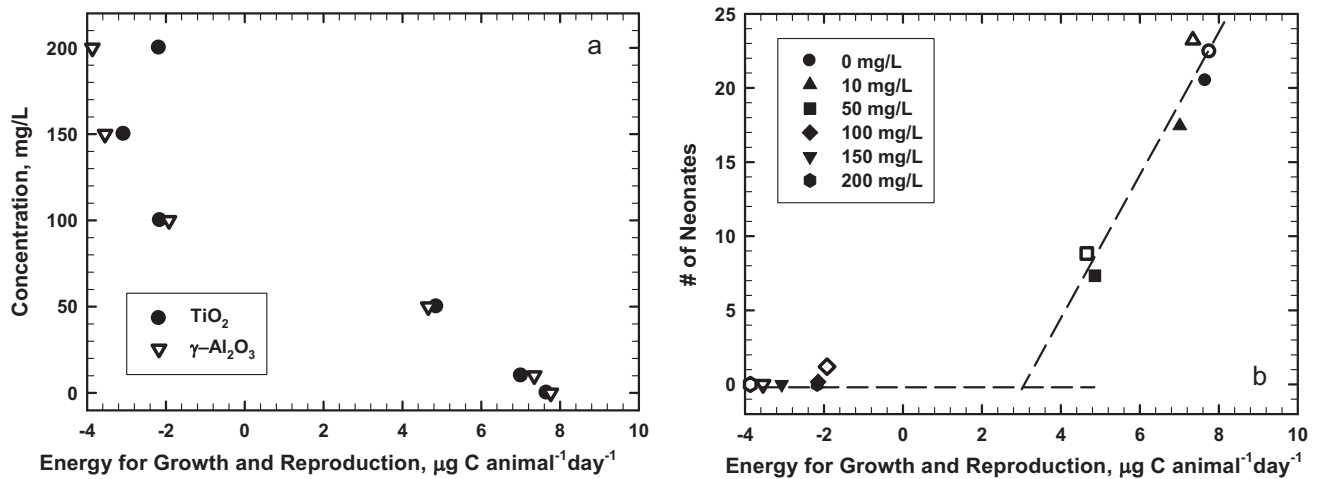
Fig. 5. (a) The relationship between concentration of nanoparticles and energy of growth and reproduction. (b) The reproductive capability of *C. dubia* as a function of energy allocated to growth and reproduction in the presence of TiO$_2$ (solid symbols) and Al$_2$O$_3$ (open symbols) nanomaterials at various concentrations. Threshold energy of 2.5–3.0 μg-C/animal/day was observed, which represented the minimal energy required for the growth of *C. dubia*.

The *Daphniidae* are also able to adjust the sexuality, population, and fitness of their offspring in response to the food conditions [27,30]. They are capable of assessing food abundance in the surrounding environment and adjust their reproductive strategies accordingly. Richman reported that, under high food supply conditions (e.g. 1×10^5 algae cells/mL/day), the energy allocated for reproduction was ca. 70%; whereas when food abundance was limited (e.g. 0.25×10^5 algae cells/mL/day), the total energy allocated for reproduce was decreased to 52% [27]. Pereira et al. showed that food abundance alone could dramatically affect the reproductive capability [30]. For *D. magna*, the total number of offspring was reduced from 82 to 29 when the food supply decreased from 1.5×10^5 to 0.75×10^5 cells/mL. The inhibition in reproduction, delay of body development, and other interruptions in body fitness observed in this study could be at least partially attributed to the fluctuation in food abundance, caused by the aggregation and settlement of nanoparticles.

Fig. 5a shows the relationship between the concentration of nanoparticles and the energy for growth and reproduction based on the measured algal cell concentrations. As the concentration of nanoparticles increased, the energy for growth and reproduction decreased due mainly to the diminishing in food supply. Fig. 5b shows the relationship between the observed reproduction and the predicted energy allocation for growth and reproduction ($S + R$). It was observed that with an increase in nanoparticle concentration, the energy used for growth and reproduction decreased accordingly, which were concurrent with decrease in total neonate number. Energy allocated for growth and reproduction was 7.7 and 7.8 μg-C/animal/day, respectively, for the control groups. The threshold energy was ca. 2.5–3.0 μg-C/animal/day, at which the animals stopped reproducing.

The predicted energy allocation pattern matched well with experimental observations. Results of reproduction experiments indicated that when the concentrations of both nanomaterials were ca. 50 mg/L, the reproduction capability of *C. dubia* was reduced by half (from 24 to 12 neonates) (Fig. 1b). The DEB model indicated that at a concentration of 50 mg/L of nanoparticles, the energy difference allocated for the growth and reproduction was close, i.e. 4.7 and 4.9 μg-C/animal/day, respectively, for TiO$_2$ and Al$_2$O$_3$. It is noted that these values are right in the middle of those of 2.5–3.0 and 7.7–7.8 μg-C/animal/day, respectively, for TiO$_2$ and Al$_2$O$_3$ when *C. dubia* stopped reproduction in the absence of nanoparticles, i.e., control.

Under optimal condition, the *Daphniidae* allocated more than 70% of assimilated energy to reproduction which was consistent with results of classic DEB studies that the growth and reproduction of aquatic animals are controlled by their energy allocation pattern [23,25]. When environmental conditions change, specifically, low food availability, *Daphniidae* reduce the energy available for reproduction as a self-adjusting mechanism for survival [27]. If the food condition becomes worse, the energy assimilated is used barely to maintain the basic body functions and the growth and reproduction activities will cease eventually. Our results indicated presence of both nanoparticles diminished the food available to *C. dubia* at EC50 concentration. Thus, the food availability and energy uptake disruption were, at least partially, contributed to the observed negative responses caused by nanoparticles.

Based on model calculations, the *C. dubia* suspended its reproduction function when the total energy allocated for growth and reproduction was reduced to around 2.5–3.0 μg-C/animal/day which corresponded to nanoparticle concentrations of between 50 and 100 mg/L (Fig. 5a). Moreover, at a particle concentration of ca. 100 mg/L, *C. dubia* showed a delay in growth. The DEB model indicates that at this concentration, the assimilation energy is less than that for maintenance. This implied that the energy obtained by the animals was barely sufficient to maintain the very basic body functions and that there was no extra energy allocated for growth and reproduction. Thus, the growth of *C. dubia* is disrupted as well, which is consistent with our experimental observations. The modeling results suggested clearly that the energy budget allocation pattern is a function of the concentration of nanomaterials. The available energy allocated for growth and reproduction is significantly decreased in the presence of nanomaterials. This energy disruption should at least be partially responsible for the adverse effects observed.

4. Conclusions

Research presented herein demonstrated no statistical difference responses of *C. dubia* were observed in the presence of same concentration of highly photoactive TiO$_2$ and a non-photocatalytic Al$_2$O$_3$. Both nanomaterials inhibited the growth of *C. dubia* at concentrations ca. >100 mg/L. The EC50 value was 42 and 45 mg/L in the presence of TiO$_2$ and Al$_2$O$_3$, respectively, based on 3-brood reproduction assay, with no statistical difference. This implies that ROS may not be totally responsible for the adverse effects experienced

by the invertebrate. Aggregation and interaction among nanoparticles, and algal cells, depletes the major food source of *Daphnia*, which plays a role on the responses of *C. dubia* to nanoparticles. It should be noted that the inhibitory concentrations of TiO_2 and Al_2O_3 for *C. dubia* were several order of magnitudes higher than the relevant concentrations of nanoparticles in environments except perhaps under special situation such as incidental spillage or discharge of nanoparticles at huge quantities to the environment [31]. Thus, under normal circumstance the potential impact of these two nanoparticles to *C. dubia* was expected to be insignificant.

Results of DEB evaluation indicated that nanoparticles could disrupt the energy of assimilation and consumption of *C. dubia* dramatically. The assimilation energy was negatively correlated to the concentration of nanomaterial, a reduction from 11 to near $0\,\mu g$-C/animal/day in the presence of TiO_2 or Al_2O_3 nanoparticles at a concentration of 200 mg/L. The energy of consumption for life-maintenance increased also with increase in the concentration of nanomaterials. Results clearly demonstrated the importance of energy disruption in determining the toxicity of nanomaterials to *C. dubia*.

Acknowledgments

Appendix A. Supplementary data

Supplementary data associated with this article can be found, in the online version, at doi:10.1016/j.jhazmat.2011.01.061.

References

[1] V.L. Colvin, The potential environmental impact of engineered nanomaterials, Nat. Biotechnol. 21 (2003) 1166–1170.
[2] S.J. Klaine, P.J.J. Alvarez, G.E. Batley, T.F. Fernandes, R.D. Handy, D.Y. Lyon, S. Mahendra, M.J. McLaughlin, J.R. Lead, Nanomaterials in the environment: behavior, fate, bioavailability, and effects, Environ. Toxicol. Chem. 27 (2008) 1825–1851.
[3] C.C Winterbourn, Reconciling the chemistry and biology of reactive oxygen species, Nat. Chem. Biol. 4 (2008) 278–286.
[4] E. Oberdorster, Manufactured nanomaterials (fullerenes, C-60) induce oxidative stress in the brain of juvenile largemouth bass, Environ. Health Perspect. 112 (2004) 1058–1062.
[5] J.E. Choi, S. Kim, J.H. Ahn, P. Youn, J.S. Kang, K. Park, J. Yi, D.Y. Ryu, Induction of oxidative stress and apoptosis by silver nanoparticles in the liver of adult zebrafish, Aquat. Toxicol. 100 (2010) 151–159.
[6] S. Tedesco, H. Doyle, J. Blasco, G. Redmond, D. Sheehan, Oxidative stress and toxicity of gold nanoparticles in *Mytilus edulis*, Aquat. Toxicol. 100 (2010) 178–186.
[7] T.M. Blickley, P. McClellan-Green, Toxicity of aqueous fullerene in adult and larval *Fundulus heteroclitus*, Environ. Toxicol. Chem. 27 (2008) 1964–1971.
[8] N. Lewinski, V. Colvin, R. Drezek, Cytotoxicity of nanoparticles, Small 4 (2008) 26–49.
[9] E. Oberdorster, S.Q. Zhu, T.M. Blickley, P. McClellan-Green, M.L. Haasch, Ecotoxicology of carbon-based engineered nanoparticles: effects of fullerene (C-60) on aquatic organisms, Carbon 44 (2006) 1112–1120.
[10] N. Shinohara, T. Matsumoto, M. Gamo, A. Miyauchi, S. Endo, Y. Yonezawa, J. Nakanishi, Is lipid peroxidation induced by the aqueous suspension of fullerene C-60 nanoparticles in the brains of *Cyprinus carpio*? Environ. Sci. Technol. 43 (2009) 948–953.
[11] T.B. Henry, F.M. Menn, J.T. Fleming, J. Wilgus, R.N. Compton, G.S. Sayler, Attributing effects of aqueous C-60 nano-aggregates to tetrahydrofuran decomposition products in larval zebrafish by assessment of gene expression, Environ. Health Perspect. 115 (2007) 1059–1065.
[12] H.-W. Chou, Nanotoxicology: from Nano Titanium Dioxide Particle Size Effect on *Ceriodaphnia dubia* to Death Mechanism, Department of Civil and Environmental Engineering, University of Delaware, Newark, DE, USA, 2008.
[13] M.H. Li, M. Boggs, T.P. Beebe, C.P. Huang, Oxidation of single-walled carbon nanotubes in dilute aqueous solutions by ozone as affected by ultrasound, Carbon 46 (2008) 466–475.
[14] L.K. Limbach, Y.C. Li, R.N. Grass, T.J. Brunner, M.A. Hintermann, M. Muller, D. Gunther, W.J. Stark, Oxide nanoparticle uptake in human lung fibroblasts: effects of particle size, agglomeration, and diffusion at low concentrations, Environ. Sci. Technol. 39 (2005) 9370–9376.
[15] X Jin, M.H. Li, J.W. Wang, C. Marambio-Jones, F.B. Peng, X.F. Huang, R. Damoiseaux, E. M.V. Hoek, High-throughput screening of silver nanoparticle stability and bacterial inactivation in aquatic media: influence of specific ions, Environ. Sci. Technol. 44 (2010) 7321–7328.
[16] M.H. Li, S. Pokhrel, X. Jin, L. Mdler, R. Damoiseaux, E.M.V. Hoek, Stability, bioavailability, and bacterial toxicity of ZnO and iron-doped ZnO nanoparticles in aquatic media, Environ. Sci. Technol. (2011).
[17] M.H Li, C.-P. Huang, Stability of oxidized single-walled carbon nanotubes in the presence of simple electrolytes and humic acid, Carbon 48 (2010) 4527–4534.
[18] M.-Y. Lin, Interactions between Titanium Dioxide Nanoparticles and Algal Cells at Moderate Particle Concentration, Civil and Environmental Department, University of Delaware, Newark, 2008, p. 98.
[19] U.S. Environmental Protection Agency, Short-Term Methods for Estimating the Chronic Toxicity of Effluents and Receiving Waters to Freshwater Organism, U.S.E.P. Agency, 2002.
[20] M. Lynch, L.J. Weider, W. Lampert, Measurement of the carbon balance in *Daphnia*, Limnol. Oceanogr. 31 (1986) 17–33.
[21] E. Mccauley, W.W. Murdoch, R.M. Nisbet, W.S.C. Gurney, The physiological ecology of *Daphnia* – development of a model of growth and reproduction, Ecology 71 (1990) 703–715.
[22] K. Rinke, J. Vijverberg, A model approach to evaluate the effect of temperature and food concentration on individual life-history and population dynamics of *Daphnia*, Ecol. Model 186 (2005) 326–344.
[23] J. Vanoverbeke, Modeling individual and population dynamics in a consumer–resource system: behavior under food limitation and crowding and the effect on population cycling in *Daphnia*, Ecol. Model 216 (2008) 385–401.
[24] S.A.L.M. Koojiman, Dynamic Energy and Mass Budgets in Biological Systems, second ed., Cambridge University Press, 2000.
[25] K. Rinke, S. Hulsmann, W.M. Mooij, Energetic costs, underlying resource allocation patterns, and adaptive value of predator-induced life-history shifts, Oikos 117 (2008) 273–285.
[26] W. Lampert, Studies on the carbon balance of *Daphnia pulex* as related to environmental conditions. II. The dependence of carbon assimilation on aminal size, temperture, food concentration and diet species, Arch. Hydrobiol. Suppl. 48 (1977) 310–335.
[27] S. Richman, The transformation of energy by *Daphnia pulex*, Ecol. Monogr. 28 (1958) 274–291.
[28] J. Urabe, Y. Watanabe, Effect of food concentration on the assimilation and production efficiencies of *Daphnia galeata* go sars (Crustacea, Cladocera), Funct. Ecol. 5 (1991) 635–641.
[29] P. Muck, W. Lampert, An experimental study on the importance of food conditions for the relative abundance of calanoid copepods and cladocerans 1. Comparative feeding studies with *Eudiaptomus gracilis* and *Daphnia longispina*, Arch. Hydrobiol. Suppl. (1984) 157–179.
[30] J.L. Pereira, F. Goncalves, Effects of food availability on the acute and chronic toxicity of the insecticide methomyl to *Daphnia* spp., Sci. Total Environ. 386 (2007) 9–20.
[31] F. Gottschalk, T. Sonderer, R.W. Scholz, B. Nowack, Modeled environmental concentrations of engineered nanomaterials (TiO_2, ZnO, Ag, CNT, fullerenes) for different regions, Environ. Sci. Technol. 43 (2009) 9216–9222.